Carborane-Based Metal–Organic Framework with High Methane and Hydrogen Storage Capacities

Robert D. Kennedy,[†] Vaiva Krungleviciute,[‡,§] Daniel J. Clingerman,[†] Joseph E. Mondloch,[†] Yang Peng,[‡,§] Christopher E. Wilmer,[⊥] Amy A. Sarjeant,[†] Randall Q. Snurr,[⊥] Joseph T. Hupp,[†] Taner Yildirim,*[‡,§] Omar K. Farha,*[†] and Chad A. Mirkin*[†]

[†]Department of Chemistry and International Institute for Nanotechnology and [⊥]Department of Chemical & Biological Engineering, Northwestern University, 2145 Sheridan Road, Evanston, Illinois 60208, United States

[‡]NIST Center for Neutron Research, National Institute of Standards and Technology, Gaithersburg, Maryland 20899, United States

[§]Department of Materials Science and Engineering, University of Pennsylvania, Philadelphia, Pennsylvania 19104, United States

S *Supporting Information*

ABSTRACT: A Cu–carborane-based metal–organic framework (MOF), **NU-135**, which contains a quasi-spherical *para*-carborane moiety, has been synthesized and characterized. **NU-135** exhibits a pore volume of 1.02 cm^3/g and a gravimetric BET surface area of ca. 2600 m^2/g, and thus represents the first highly porous carborane-based MOF. As a consequence of the unique geometry of the carborane unit, **NU-135** has a very high volumetric BET surface area of ca. 1900 m^2/cm^3. CH_4, CO_2, and H_2 adsorption isotherms were measured over a broad range of pressures and temperatures and are in good agreement with computational predictions. The methane storage capacity of **NU-135** at 35 bar and 298 K is ca. 187 v_{STP}/v. At 298 K, the pressure required to achieve a methane storage density comparable to that of a compressed natural gas (CNG) tank pressurized to 212 bar, which is a typical storage pressure, is only 65 bar. The methane working capacity (5–65 bar) is 170 v_{STP}/v. The volumetric hydrogen storage capacity at 55 bar and 77 K is 49 g/L. These properties are comparable to those of current record holders in the area of methane and hydrogen storage. This initial example lays the groundwork for carborane-based materials with high surface areas.

KEYWORDS: *carborane, boron, MOF, metal–organic framework, coordination polymer, porous, hydrogen, methane*
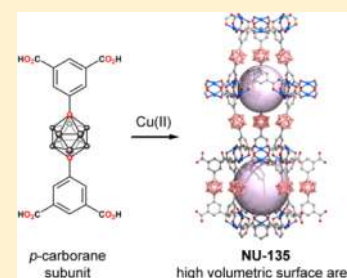
INTRODUCTION

Nanoporous materials such as metal–organic frameworks (MOFs) with tailorable pore volumes, high internal surface areas,[1,2] and chemical diversity form an important emerging class of materials that are potentially useful in a wide range of applications including ion exchange,[3] catalysis,[4,5] gas separation,[6–8] sensing,[9] and storage.[10–12] In particular, MOFs have attracted great interest for onboard hydrogen and methane storage in vehicles, which is a long-standing goal for those interested in energy independence and the protection of the environment. Over the past decade, significant progress has been made toward building new classes of MOFs with desired material characteristics. This has been achieved via, for example, the tailoring of pore geometry, volume, surface area, and density, and by the incorporation of unsaturated metal centers.[13,14] Control over these parameters is crucial for realizing materials with high gas uptake capacity.

Polyhedral boranes and heteroboranes are a unique class of cluster compounds with properties and geometries that are not accessible with carbon-based systems.[15] Among the polyhedral boranes, the family of isomeric icosahedral dicarbaboranes ($closo$-$C_2B_{10}H_{12}$)[15] and their metallo-derivatives[16] have received much attention because of their varied chemistry,[17] redox properties,[18] thermal stability, and their potential for applications in the areas of medicine[19] and materials

chemistry.[15] Recently we reported a series of MOFs that are derived from $closo$-1,12-$C_2B_{10}H_{12}$ (*para*-carborane). The carborane-based MOFs displayed exceptional thermal stability and large CO_2/CH_4 and CO_2/N_2 adsorption selectivities.[7,8,20–22] However, the pore volumes and internal surface areas of these carborane-based MOFs were relatively small, thus limiting their usefulness in gas storage applications. Here we report a new copper(II)–carborane-based MOF in which the unique icosahedral structure of the carborane-derived ligand core leads to a combination of pore volume and high volumetric surface area that is conducive to high methane and hydrogen storage capacities.

RESULTS AND DISCUSSION

To create a new carborane-based MOF with a large pore volume and surface area, a relatively long boron-rich ligand was synthesized that consists of a central *p*-carborane unit and two isophthalic acid groups (**LH₄**)(Scheme 1). It has been shown that organic-based bis(isophthalic acid) ligands of this type produce an isoreticular family of copper(II)-based MOFs, known as the NOTT-100 series, with the **nbo** topology.[23–28]

Scheme 1. Synthesis of the Carborane—Bis(isophthalic acid) Ligand (LH₄) Used to Construct NU-135.[a]
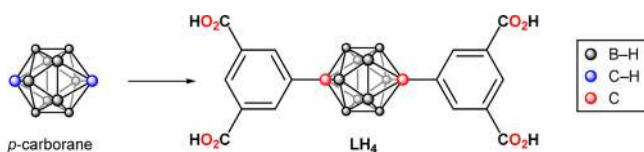
[a]Reaction conditions: (i) *n*-BuLi, THF; CuCl, THF −40 to 70 °C; diethyl 5-iodoisophthalate, Pd(PPh₃)₄, NMP, 100 °C, 16 h (42%). (ii) LiOH (1 M), THF/H₂O 2:1, rt, 36 h; H₃O⁺ (84%).

This family of MOFs shows great promise in the areas of methane and hydrogen storage. The extended carborane-based ligand **LH₄** was synthesized via Cu(I)−Pd(II) coupling chemistry adapted from a report by Schöberl et al.[29] The synthesis and characterization are described in the Supporting Information. The solvothermal reaction between Cu(NO₃)₂· 2.5H₂O and **LH₄** in DMF at 80 °C for 16 h yielded blue crystals (**NU-135**). Single-crystal X-ray diffraction analysis revealed that **NU-135** crystallizes in the $R\bar{3}m$ space group and has the **nbo** topology (Figure 1). The framework nodes consist of Cu₂ units coordinated by the carboxylate groups of **L**$^{4-}$ in a paddlewheel configuration. As synthesized, each axial coordination site is occupied by a water molecule. The network is noncatenated, and there are two distinct cages, each with D_{3d} symmetry, as shown in Figure 1b. Importantly, the *p*-carborane moieties, which are approximately equal in length to a phenylene group, are quasi-spherical and project into the pores of the framework. This has important implications regarding surface area, pore volume, and gas uptake (vide infra). The experimental unit cell dimensions are $a = b =$ 18.6953(7) Å and $c = 39.1379(17)$ Å. The solvent-free structure of **NU-135** has a density of 0.751 g/cm³. This value is used to convert the measured hydrogen and methane storage capacities to volumetric units (vide infra). The crystallographically derived structure was used to simulate N₂, CH₄, CO₂, and H₂ gas adsorption (see the Supporting Information for simulation details).

After the guest solvent molecules were removed via supercritical CO₂ (see the Supporting Information for activation details),[30,31] the samples were further activated thermally by heating slowly to 100 °C for 3−5 h under dynamic vacuum. The porosity was determined by nitrogen adsorption at 77 K as shown in Figure 2. The experimental and calculated Brunauer−Emmett−Teller[32] (BET) surface areas are 2530 and 2700 m²/g, respectively. The pore volume of **NU-135**, derived from the measured N₂ isotherm, is 1.02 cm³/g (77% empty space), which is somewhat higher than the calculated value of 0.9 cm³/g (68% porosity) by PLATON.[33,34] Nevertheless, the nitrogen isotherm measurements were repeated on several batches of samples using different apparatus (Quantachrome) in addition to our custom high-pressure Sievert and essentially identical results were obtained (see Figure S9 in the Supporting Information).

Because of the close similarities in unit-cell parameters, direct comparisons may be drawn between **NU-135** and members of the isoreticular family of MOFs based on *p*-phenylene bis(isophthalic acid)s known as the NOTT-100 series.[23] As mentioned above, the *p*-carborane moiety is approximately equal in length to a phenylene group and, consequently, the unit-cell volume of **NU-135** is only 2.5% greater than that of terphenyl derivative NOTT-101. Importantly, the volumetric
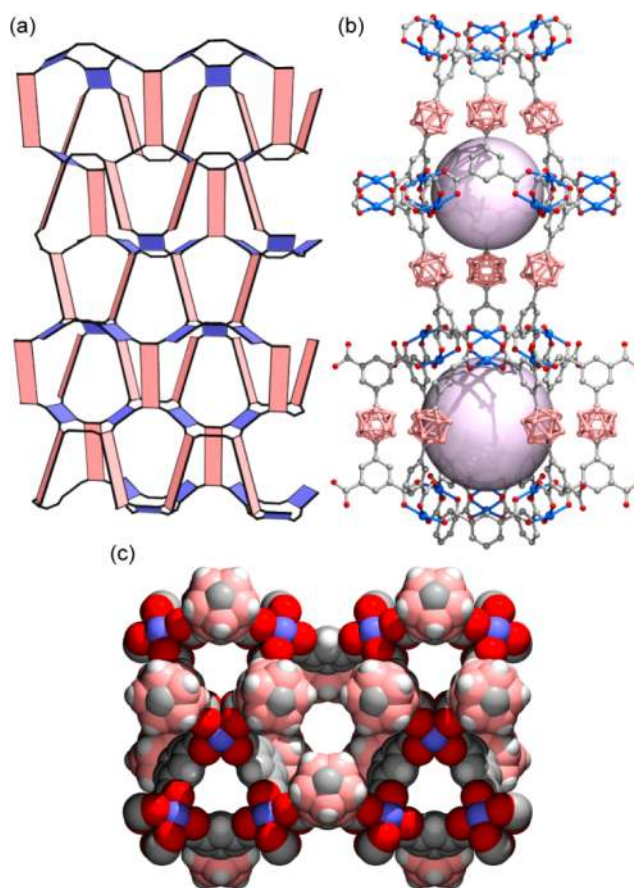

Figure 1. Representations of the crystal structure of **NU-135**. (a) Simplified **nbo** network viewed along the *ab* plane. Blue squares = Cu₂ paddlewheels; pink rectangles = carborane bis(isophthalic acid) ligands. (b) Detail of pores, viewed along the *ab* plane. Lilac spheres indicate the largest sphere-shaped voids that can be found within the evacuated MOF as defined by the internal van der Waals surface of the material. Hydrogen atoms removed for clarity. (c) Space-filling representation, viewed along the *c* axis, illustrating the carborane-lined pores. Atom code: C = gray; H = white; O = red; B = pink; Cu = blue.

surface area (via BET measurement) is ca. 30% greater (i.e., 1900 and 1460 m²/cm³ for **NU-135** and NOTT-101, respectively),[23,28] yet the crystallographically derived fraction of free space within **NU-135** (68%) is only slightly smaller than that of NOTT-101 (71%). These differences in geometry are a consequence of the globular *p*-carborane subunit. It is important to note here that this effect seems unique to the incorporation of the carborane unit. For comparison, the addition of two or four methyl substituents to the central phenylene group of NOTT-101, to produce NOTT-106 and -107,[23,25] respectively, reduces the fraction of free space within the frameworks, as expected. However, the addition of the methyl groups also significantly reduces the volumetric surface area (e.g., 1460 and 1340 m²/cm³ for NOTT-101 and NOTT-107, respectively).

Temperature-dependent high-pressure adsorption measurements were performed at the Center for Neutron Research, National Institute of Standards and Technology (NIST), using a computer-controlled Sieverts apparatus, the details of which have been published elsewhere[35] and are briefly discussed in the Supporting Information. The gas uptake properties of **NU-135** at 298 K for N₂, CO₂, and CH₄ are shown in Figure 3.
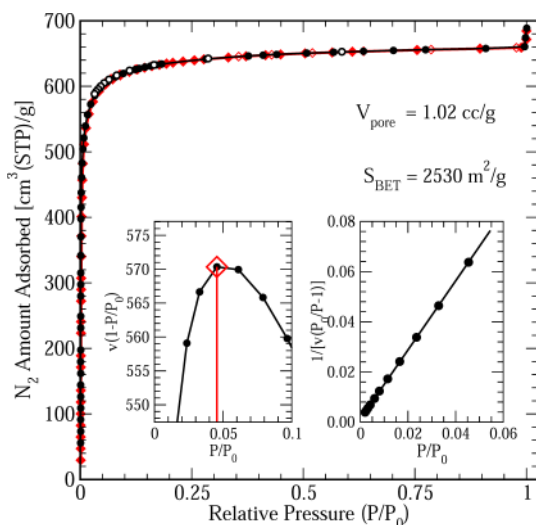
Figure 2. Nitrogen isotherms for **NU-135** at 77 K before (black) and after (red) CH_4, CO_2, and H_2 adsorption measurements, indicating no sample degradation over the course of the adsorption cycles. The inset on the left shows the consistency plot used to determine the pressure range for BET fitting, which is shown in the inset on the right.
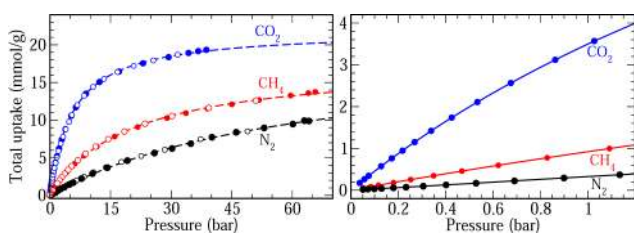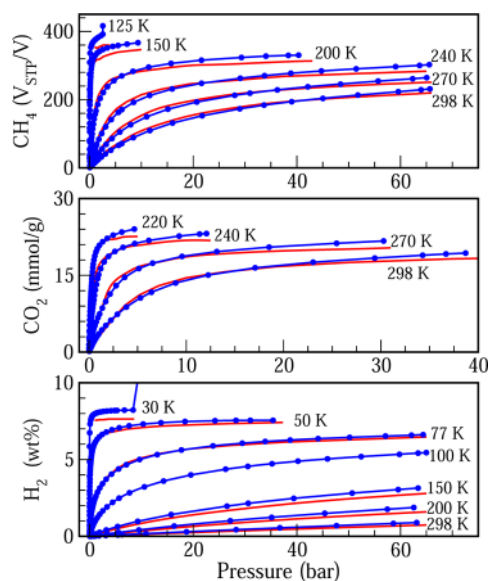

Figure 3. Left: High-pressure gas adsorption measurements on **NU-135** for CO_2, CH_4, and N_2 at 298 K. The dashed-lines are a simple one-site Langmuir fit to the data. Right: Low-pressure ranges of the isotherms, indicating large CO_2/CH_4 and CO_2/N_2 selectivities.

Although the previously reported carborane-based MOFs exhibited low total gas uptake, they exhibited large CO_2/CH_4 selectivities of up to 17 at 0.5 bar. **NU-135** exhibits much larger total gas uptake compared to earlier carborane-based MOFs but the CO_2/CH_4 selectivity is reduced to ca. 4 at 0.5 bar (Figure 3). In the case of CO_2/N_2 selectivity, **NU-135** exhibits a relatively large value of 14.5 at 0.15 bar, which could be important for carbon capture applications from flue-gas. As shown in Figure 3, **NU-135** exhibits a high capacity for methane at high pressures. This capacity is comparable to MOFs that exhibit high methane storage, such as UTSA-20,[36] PCN-14,[24] NU-111,[37] and NU-125.[38] We observed an absolute methane storage capacity of 230 v_{STP}/v (i.e., ca. 10.3 mmol/cm^3 or 13.7 mmol/g) at 65 bar, which corresponds to the amount of methane stored in a CNG tank at 212 bar.[39] Thus, **NU-135** effectively reduces the pressure required for useful loading (230 v_{STP}/v) by a factor of 3.3, down to 65 bar. This is a potentially important advance as it demonstrates the ability of a material to absorb natural gas to the extent where it may become commercially attractive. The stability of **NU-135** toward multiple cycles of methane adsorption/desorption was tested (see Figure S14 in the Supporting Information). There is no sample degradation at 35 or 65 bar over eight cycles, and the variation of the total adsorption at 65 bar is less than 1.5%, which is within the error of the measurements.

Ultimately, the deliverable methane capacity determines the driving range of a natural gas vehicle (NGV). In this case it is important for a porous material to have low capacity in the ca. 5 bar range, and high capacity in the 60−70 bar range.[40] The adsorption isotherm of **NU-135** has a relatively shallow gradient at low pressure; taking 5 bar as the specific lower pressure limit and 65 bar as the upper limit, the deliverable capacity of **NU-135** is ca. 170 v_{STP}/v at 298 K (Figure 3). This value is comparable to MOFs that show the most promise for deliverable methane storage (e.g., UTSA-20 and PCN-14).[24,35,37,38] These properties may arise from the icosahedral carborane unit which provides an almost ideal balance between surface area, pore size and pore volume. Furthermore, it is reasonable to suggest that the inverted polarity of the B−H bonds and correspondingly hydridic nature of the carborane-bound hydrogen atoms impart properties to the framework that are not accessible via regular hydrocarbon chemistry.

In addition to performing high-pressure isotherm measurements at 298 K, we also measured high-pressure CH_4 adsorption over a wide range of temperatures on the same sample (Figure 4). Low temperature adsorption isotherm


Figure 4. Experimental (blue) and simulated (red) high-pressure absolute gas adsorption isotherms for **NU-135** at several temperatures.

measurements are indispensable because they provide information on the maximum gas storage capacity of the material. For **NU-135**, we obtained a maximum methane uptake of ca. 392 v_{STP}/v (23.3 mmol/g) at 125 K, which effectively corresponds to the upper limit for the amount of gas that can be adsorbed under very large external pressures at ambient temperature. The observed maximum CH_4 uptake is very close to the upper limit of 432 v_{STP}/v (25.7 mmol/g) as obtained from taking the nitrogen-based pore volume and assuming liquid methane density at 125 K. This suggests that methane is able to access most of the pores in **NU-135** that are accessible to nitrogen at 77 K.

CO_2, and H_2 adsorption isotherms were also measured over similarly wide pressure and temperature ranges (see Figure 4). The maximum excess H_2 uptake at 77 K is about 5.1 wt % (see Figure S13 in the Supporting Information), which is in good agreement with that expected from "Chahine's rule"[41] (i.e., 1 wt % for every 500 m^2/g). This empirical rule is observed for

most carbon or carbon-rich nanoporous materials in which van der Waals interactions are the dominant mechanism for adsorption. In terms of absolute volumetric hydrogen uptake, an impressive maximum value of ca. 49 g/L is obtained above ca. 55 bar at 77 K. This value places **NU-135** among the highest performing MOFs for volumetric hydrogen storage.[10] **NU-135** also exhibits significant CO_2 uptake at high pressures. The maximum CO_2 uptake at 220 K is 24.6 mmol/g, which is in good agreement with the upper limit of 27.2 mmol/g as estimated from the nitrogen pore volume and liquid density of CO_2 at this temperature. The CO_2 uptake at room temperature and 30 bar is ca. 18.5 mmol/g, corresponding to 75% of the total pore volume. At 0.15 bar and 298 K (i.e., a condition that approximates flue gas from coal power plants), the CO_2 uptake is about 3 wt %. This value is lower than that of MOF-74, which contains open metal sites, but higher than the uptakes exhibited by many MOFs reported in a recent CO_2 screening survey.[42] The simulated isotherms for H_2, CH_4, and CO_2 are in good agreement with the experimental isotherms (Figure 4).

The natures of the adsorption sites and gas−framework interactions in **NU-135** were probed by using the Clausius−Clapeyron equation to extract the isosteric heats of adsorption (Q_{st}) from the absolute isotherms measured at different temperatures (Figure 5, details in the Supporting Informa-
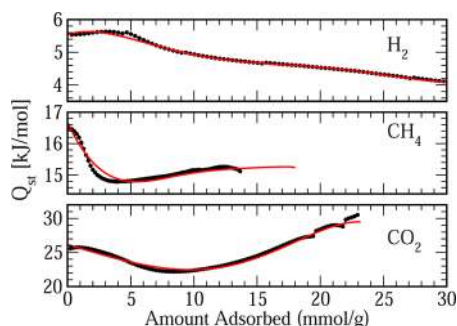
Figure 5. Isosteric heats of adsorption (Q_{st}) as a function of gas loading in mmol(gas)/g(**NU-135**). The red lines are from virial fitting. The black dotted lines are from original isotherm data with spline (without any fitting).

tion).[1] The magnitudes of the Q_{st} values are comparable with other Cu−paddlewheel-based MOFs.[23,35] In the cases of CO_2 and CH_4, the Q_{st} values are initially high, drop, and then increase. This is probably due to significant gas−gas interactions which become important at higher loading. In the case of hydrogen, the Q_{st} stays constant initially (ca. 5.6 kJ/mol) and then decreases to ca. 4 kJ/mol at greater H_2 loadings. This may be due to negligible H_2−H_2 interactions.

CONCLUSIONS

The interplay between volumetric surface area and pore volume makes an important contribution to volumetric adsorption in MOFs. Icosahedral carboranes possess a unique quasi-spherical geometry that is inaccessible using organic chemistry, and can thus be used to create MOFs with pore geometries that cannot be obtained using organic ligands. Thus, compared to an isostructural MOF that contains a phenylene group rather than a *p*-carborane group, **NU-135** has a slightly reduced pore volume but greatly enhanced volumetric surface area. This is reflected by the exceptionally high volumetric hydrogen and methane uptake exhibited by **NU-135**. An important aspect of

this work is the ease with which the carborane subunit may be incorporated into larger structures. This allows for specific frameworks, in this case the isoreticular NOTT-100 series, to be targeted and modified with the carborane subunit in order to increase the volumetric surface area. **NU-135**, which was synthesized via this approach, has approximately twice the pore volume and surface area of previously reported carborane-based MOFs, and thus represents the first highly porous carborane-based MOF. The incorporation of the carborane polyhedra into other high-performance MOFs is an exciting prospect, and will hopefully lead to materials with record-breaking gas sorption properties. Furthermore, the simulations agree very well with the experimental measurements over a wide pressure and temperature range, as well as across several different sorbate molecules, thus demonstrating the applicability of simulations in the cases of MOFs that contain exotic components such as polyhedral carboranes. This novel strategy, in which a carborane moiety is employed to greatly increase volumetric surface area, will allow us and others to expand the current capability of porous materials for gas storage applications.

ASSOCIATED CONTENT

Ⓢ Supporting Information

General procedures, materials, and instrumentation; synthesis, characterization (^1H, ^{13}C, ^{11}B NMR, HR-MS, elemental analysis), and crystallographic information files (CIF) for **LH$_4$**, **LEt$_4$**, and **NU-135**; PXRD, adsorption excess isotherms, BET analysis, and simulation details; support disclaimers. This material is available free of charge via the Internet at http://pubs.acs.org.

AUTHOR INFORMATION

Corresponding Author

*E-mail: chadnano@northwestern.edu (C.A.M.); o-farha@northwestern.edu (O.K.F.); taner@seas.upenn.edu (T.Y.).

Author Contributions

R.D.K. and T.Y. contributed equally to this work.

Notes

The authors declare the following competing financial interest: O.K.F., C.E.W., R.Q.S., and J.T.H. hold equity interests in NuMat Technologies, a company that is pursuing commercialization of MOFs for methane storage.

ACKNOWLEDGMENTS

■ REFERENCES

(1) Farha, O. K.; Eryazici, I.; Jeong, N. C.; Hauser, B. G.; Wilmer, C. E.; Sarjeant, A. A.; Snurr, R. Q.; Nguyen, S. T.; Yazaydın, A. Ö.; Hupp, J. T. *J. Am. Chem. Soc.* **2012**, *134*, 15016−15021.

(2) Sarkisov, L. *Adv. Mater.* **2012**, *24*, 3130−3133.

(3) Min, K. S.; Suh, M. P. *J. Am. Chem. Soc.* **2000**, *122*, 6834−6840.

(4) Lee, J.; Farha, O. K.; Roberts, J.; Scheidt, K. A.; Nguyen, S. T.; Hupp, J. T. *Chem. Soc. Rev.* **2009**, *38*, 1450−1459.

(5) Ma, L.; Abney, C.; Lin, W. *Chem. Soc. Rev.* **2009**, *38*, 1248−1256.

(6) Li, J.-R.; Kuppler, R. J.; Zhou, H.-C. *Chem. Soc. Rev.* **2009**, *38*, 1477−1504.

(7) Bae, Y.-S.; Farha, O. K.; Spokoyny, A. M.; Mirkin, C. A.; Hupp, J. T.; Snurr, R. Q. *Chem. Commun.* **2008**, 4135−4137.

(8) Bae, Y.-S.; Spokoyny, A. M.; Farha, O. K.; Snurr, R. Q.; Hupp, J. T.; Mirkin, C. A. *Chem. Commun.* **2010**, *46*, 3478−3480.

(9) Kreno, L. E.; Leong, K.; Farha, O. K.; Allendorf, M.; Van Duyne, R. P.; Hupp, J. T. *Chem. Rev.* **2012**, *112*, 1105−1125.

(10) Suh, M. P.; Park, H. J.; Prasad, T. K.; Lim, D.-W. *Chem. Rev.* **2012**, *112*, 782−835.

(11) Farha, O. K.; Yazaydın, A. Ö.; Eryazici, I.; Malliakas, C. D.; Hauser, B. G.; Kanatzidis, M. G.; Nguyen, S. T.; Snurr, R. Q.; Hupp, J. T. *Nat. Chem.* **2010**, *2*, 944−948.

(12) Furukawa, H.; Ko, N.; Go, Y. B.; Aratani, N.; Choi, S. B.; Choi, E.; Yazaydın, A. Ö.; Snurr, R. Q.; O'Keeffe, M.; Kim, J.; Yaghi, O. M. *Science* **2010**, *329*, 424−428.

(13) Sumida, K.; Stück, D.; Mino, L.; Chai, J.-D.; Bloch, E. D.; Zavorotynska, O.; Murray, L. J.; Dincă, M.; Chavan, S.; Bordiga, S.; Head-Gordon, M.; Long, J. R. *J. Am. Chem. Soc.* **2013**, *135*, 1083−1091.

(14) Wu, H.; Zhou, W.; Yildirim, T. *J. Am. Chem. Soc.* **2009**, *131*, 4995−5000.

(15) Grimes, R. N. *Carboranes*, second ed.; Elsevier: Amsterdam, 2011.

(16) Hawthorne, M. F.; Young, D. C.; Andrews, T. D.; Howe, D. V.; Pilling, R. L.; Pitts, A. D.; Reintjes, M.; Warren, L. F.; Wegner, P. A. *J. Am. Chem. Soc.* **1968**, *90*, 879−896.

(17) Wedge, T. J.; Hawthorne, M. F. *Coord. Chem. Rev.* **2003**, *240*, 111−128.

(18) Lee, M. W.; Farha, O. K.; Hawthorne, M. F.; Hansch, C. H. *Angew. Chem., Int. Ed.* **2007**, *46*, 3018−3022.

(19) Valliant, J. F.; Guenther, K. J.; King, A. S.; Morel, P.; Schaffer, P.; Sogbein, O. O.; Stephenson, K. A. *Coord. Chem. Rev.* **2002**, *232*, 173−230.

(20) Farha, O. K.; Spokoyny, A. M.; Mulfort, K. L.; Galli, S.; Hupp, J. T.; Mirkin, C. A. *Small* **2009**, *5*, 1727−1731.

(21) Farha, O. K.; Spokoyny, A. M.; Mulfort, K. L.; Hawthorne, M. F.; Mirkin, C. A.; Hupp, J. T. *J. Am. Chem. Soc.* **2007**, *129*, 12680−12681.

(22) Spokoyny, A. M.; Farha, O. K.; Mulfort, K. L.; Hupp, J. T.; Mirkin, C. A. *Inorg. Chim. Acta* **2010**, *364*, 266−271.

(23) Yan, Y.; Lin, X.; Yang, S.; Blake, A. J.; Dailly, A.; Champness, N. R.; Hubberstey, P.; Schröder, M. *Chem. Commun.* **2009**, 1025−1027.

(24) Ma, S.; Sun, D.; Simmons, J. M.; Collier, C. D.; Yuan, D.; Zhou, H.-C. *J. Am. Chem. Soc.* **2007**, *130*, 1012−1016.

(25) Wilmer, C. E.; Leaf, M.; Lee, C. Y.; Farha, O. K.; Hauser, B. G.; Hupp, J. T.; Snurr, R. Q. *Nature Chem.* **2011**, *4*, 83−89.

(26) Chen, B.; Ockwig, N. W.; Millward, A. R.; Contreras, D. S.; Yaghi, O. M. *Angew. Chem., Int. Ed.* **2005**, *44*, 4745−4749.

(27) Hu, Y.; Xiang, S.; Zhang, W.; Zhang, Z.; Wang, L.; Bai, J.; Chen, B. *Chem. Commun.* **2009**, 7551−7553.

(28) Lin, X.; Jia, J.; Zhao, X.; Thomas, K. M.; Blake, A. J.; Walker, G. S.; Champness, N. R.; Hubberstey, P.; Schröder, M. *Angew. Chem., Int. Ed.* **2006**, *45*, 7358−7364.

(29) Schöberl, U.; Magnera, T. F.; Harrison, R. M.; Fleischer, F.; Pflug, J. L.; Schwab, P. F. H.; Meng, X.; Lipiak, D.; Noll, B. C.; Allured, V. S.; Rudalevige, T.; Lee, S.; Michl, J. *J. Am. Chem. Soc.* **1997**, *119*, 3907−3917.

(30) Farha, O. K.; Hupp, J. T. *Acc. Chem. Res.* **2010**, *43*, 1166−1175.

(31) Nelson, A. P.; Farha, O. K.; Mulfort, K. L.; Hupp, J. T. *J. Am. Chem. Soc.* **2008**, *131*, 458−460.

(32) Brunauer, S.; Emmett, P. H.; Teller, E. *J. Am. Chem. Soc.* **1938**, *60*, 309−319.

(33) Spek, A. L. *Acta Crystallogr., Sect. D* **2009**, *65*, 148−155. The van der Waals radii used in the analysis: C, 1.70; H, 1.2; B, 1.63; Cu, 1.4; N, 1.5; O, 1.52.

(34) This result is not unexpected, as crystallographically derived porosities often underestimate those obtained via adsorption experiments by up to 20%.

(35) Zhou, W.; Wu, H.; Hartman, M. R.; Yildirim, T. *J. Phys. Chem. C* **2007**, *111*, 16131−16137.

(36) Guo, Z.; Wu, H.; Srinivas, G.; Zhou, Y.; Xiang, S.; Chen, Z.; Yang, Y.; Zhou, W.; O'Keeffe, M.; Chen, B. *Angew. Chem., Int. Ed.* **2011**, *50*, 3178−3181.

(37) Peng, Y.; Srinivas, G.; Wilmer, C. E.; Eryazici, I.; Snurr, R. Q.; Hupp, J. T.; Yildirim, T.; Farha, O. K. *Chem. Commun.* **2013**, *49*, 2992−2994.

(38) Wilmer, C. E.; Farha, O. K.; Yildirim, T.; Eryazici, I.; Krungleviciute, V.; Sarjeant, A. A.; Snurr, R. Q.; Hupp, J. T. *Energy Environ. Sci.* **2013**, *6*, 1158−1163.

(39) The definition of STP used in this paper is 273 K and 1 atm, 1 mmol/g means 22.414 cm^3/g.

(40) Makal, T. A.; Li, J.-R.; Lu, W.; Zhou, H.-C. *Chem. Soc. Rev.* **2012**, *41*, 7761−7779.

(41) Poirier, E.; Chahine, R.; Bose, T. K. *Int. J. Hydrogen Energy* **2001**, *26*, 831−835.

(42) Yazaydın, A. Ö.; Snurr, R. Q.; Park, T.-H.; Koh, K.; Liu, J.; LeVan, M. D.; Benin, A. I.; Jakubczak, P.; Lanuza, M.; Galloway, D. B.; Low, J. J.; Willis, R. R. *J. Am. Chem. Soc.* **2009**, *131*, 18198−18199.